Journal of Natural Gas Science and Engineering 34 (2016) 85–99

Contents lists available at ScienceDirect

Journal of Natural Gas Science and Engineering

journal homepage: www.elsevier.com/locate/jngse

The influence of structure parameters on stress of plate-fin structures in LNG heat exchanger

Hongqiang Ma [a, c, *], Caiqin Hou [a, **], Rongxia Yang [a], Chune Li [a], Bingshan Ma [a, ***], Junqiang Ren [b], Yemin Liu [a]

[a] School of Civil Engineering, Lanzhou University of Technology, Lanzhou, China
[b] State Key Lab Adv Proc & Recycling Nonferrous Met, Lanzhou University of Technology, Lanzhou, China
[c] Sinopec Petroleum Engineering Zhongyuan Corporation, Puyang, China

ARTICLE INFO

Article history:
Received 3 April 2016
Received in revised form
17 June 2016
Accepted 21 June 2016
Available online 23 June 2016

Keywords:
LNG
Plate-fin structure
Stress
Safety
Finite element method

ABSTRACT

In order to ensure the structural safety of plate-fin structures in actual operation process and guide the structural design of LNG plate-fin heat exchanger, the influence of structure parameters was investigated on stress of plate-fin structures based on Finite Element Method and thermal elastic theory. The results show that the stress is complex at the brazed joints in actual operation process of LNG PFHE and the equivalent stress will reach the peak value at brazed joint near fin side due to the influence of the direct stress in *y* direction. Meanwhile, the peak value of equivalent stress in plate-fin structures is slightly impacted by the fin height and plate thickness and is obviously impacted by the brazing seam thickness, fin thickness and fin distance. The influence of the brazing seam thickness, fin thickness and fin distance for that is mainly induced by the direct stress in *y* direction. These results will provide some constructive instructions in the structural design for plate-fin heat exchanger in a large-scale LNG cold-box.

1. Introduction

Plate-fin heat exchanger (PFHE), as a type of compact exchangers, has been widely used in the liquid natural gas (LNG) plant (Kuznetsov and Shamirzaev, 2007; Liu and Winterton, 1991). Currently, the aluminum PFHE has been mainly used in small-scale LNG plants while rarely in large-scale LNG plants as main cryogenic heat exchanger in the world (Ligterink et al., 2012). Plate-fin structures, as the key component of PFHE, will cause severe stress damage if the design is unreasonable for structure parameters of LNG PFHE in a large-scale LNG cold-box. This may influence the safe operation of PFHE in a large-scale cold-box. However, the stress phenomenon in plate-fin structures is still a long way from being understood due to the complexity of that and the lack of research work in this field.

At present, many investigations have been carried out in order to investigate the behavior of stress in plate-fin structures. However, most of the investigations have focused on residual stress in brazing process (Aiyangar et al., 2005; Chang and Lee, 2007; Galli et al., 2006; Liu, 1997); for example, the brazed residual stress and its influencing factors were analyzed to optimize the brazing technology for 304 stainless steel plate-fin structures (Jiang et al. 2010, 2011a, 2011b, 2011c, 2012). The results showed that the slow-cooling method can greatly improve the brazing performance of plate-fin structures (Chen et al., 2006). At the same time, in Chena et al. (2005) and Xie and Ling (2010) study, the residual stress was also analyzed for plate-fin structures in the brazing process based on thermal elastic-plastic theory. The results obtained by numerical simulation based on finite element method (FEM) indicated that the residual stress is extremely complex at the brazed joint, and high residual stress would have significant influence on the quality of PFHE. With these results, it is suggested that FEM, which is an effective method, is widely used to predict the stress of plate-fin structures (Brown et al., 2006; Celik et al., 2007; Civalek, 2004).

Meanwhile, the stress was also analyzed for plate-fin structures in actual operation process of LNG PFHE based on FEM and thermal

* Corresponding author. School of Civil Engineering, Lanzhou University of Technology, Lanzhou, China.
** Corresponding author. School of Civil Engineering, Lanzhou University of Technology, Lanzhou, China.
*** Corresponding author. School of Civil Engineering, Lanzhou University of Technology, Lanzhou, China.
E-mail addresses: mhq2014@sina.com (H. Ma), zjshcqzxy@163.com (C. Hou), mbs1010@126.com (B. Ma).

http://dx.doi.org/10.1016/j.jngse.2016.06.050
1875-5100/

elastic theory in our previous work. For example, the stress concentration and structural damage may occur in the plate-fin structures of LNG PFHE if the operation process is unreasonable in large-scale LNG plants. Therefore, in order to investigate the stress characteristic of LNG PFHE in the operation process of large-scale LNG plants, the influence of operation parameters was analyzed for the stress of plate-fin structures in actual operation process (Ma et al., 2015). According to the result, the peak value of equivalent stress is obviously impacted by the temperature difference between natural gas (NG) and mixture refrigerant (MR) and slightly influenced by the heat exchange performance of LNG PFHE when the temperature difference between NG and MR is no more than 5 K in actual operation process. Also, the peak value of equivalent stress is also significantly impacted by the NG pressure while slightly influenced by the MR pressure. At present, for the PFHE in a large-scale LNG cold-box, the operating procedure in the cool-down and heat-up process draws lessons from that in a small-scale LNG cold-box. The cool-down and heat-up processes are operated by virtue of controlling the temperature changing rate of NG or MR and temperature difference between NG and MR within PFHE. Severe stress concentration and thermal shocking will be caused in plate-fin structures if the operation procedure on the temperature difference between NG and MR and the temperature changing rate of NG or MR is unreasonable in the cool-down and heat-up process. This may influence safety of PFHE in a large-scale cold-box. Therefore, the stress characteristic of plate-fin structures was also analyzed in the cool-down and heat-up process of LNG PFHE in a large-scale LNG cold-box (Ma et al. 2014, 2016). Based on the results, the equivalent stress and direct stresses change rapidly and consistently reach the peak value in the brazed joint, and a crack will initiate in this region in the cool-down and heat-up process of LNG PFHE in a large-scale LNG cold-box. The peak value of equivalent stress in plate-fin structures steadily increases with the increase of temperature difference between NG and MR. At the same time, the peak value of equivalent stress is slightly impacted by the temperature changing rate as the temperature changing rate of NG is the same as that of MR in the cool-down and heat-up process.

Although the stress phenomenon of plate-fin structures has been investigated in operation process of LNG PFHE in large-scale LNG cold-box, it is still lack for the influence of structure parameters on the stress of plate-fin structures in LNG PFHE. Plate-fin structures could cause severe stress damage if the design is unreasonable for the structure parameters of LNG PFHE in a large-scale LNG cold-box. Therefore, in order to aid the structure design of LNG PFHE and ensure safe operation of plate-fin structures in LNG PFHE of large-scale LNG cold-boxes, it is needed to investigate the influence of structure parameters for the stress of plate-fin structures based on the thermal elastic theory.

According to the references (Kim and Kuwamura, 2007; Kong et al., 2008; Sen et al., 2007), the numerical simulation based on finite element method will be a useful tool to predict the stress phenomenon of plate-fin structures. In this work, a finite element method was adopted to investigate the stress of plate-fin structures in actual operation process of LNG PFHE in a large-scale LNG cold-box. The stress distributions of plate-fin structures were analyzed in the MR outlet of LNG PFHE. At the same time, the influence of structure parameters was investigated on the stress of plate-fin structures in the actual operation process of LNG PFHE in a large-scale LNG cold-box. A method was proposed to improve the structural strength of plate-fin structures in LNG PFHE of large-scale LNG cold-box.

2. Analysis of strength theory

At the present stage, many investigations show that the structural damage is induced by the two types: brittle fracture and plastic yield. For the plastic material, the structural damage is mainly induced by the plastic yield. Similarly, the brittle fracture is the main reason to induce the structural damage for the brittle material. As for plate-fin structures in complex stress state, the plastic yield is a major reason of structural damage because that the plate-fin structures consist of aluminum alloy which is plastic material. In other words, the plastic yield is not allowed for plate-fin structures in actual operation process of LNG PFHE. In order to ensure the structural safety of plate-fin structures in actual operation process, a criterion is needed to evaluate whether the stress of plate-fin structures is more than the yield limit or not. According to literature (Lee, 1988; Ma et al., 2015), the Von Mises yield criterion is the fundamental criterion to judge whether the plastic yield failure occurs in plate-fin structures or not. Based on the yield criterion, the plastic deformation which induces the plastic yield failure of plate-fin structures may occur in actual operation process when the equivalent stress (von Mises stress) is more than the allowable stress, whereas the elastic deformation will occur. In other words, the plastic yield failure may occur when the equivalent stress is more than the allowable stress. At the same time, according to this evaluation standard on structure cracking, the initial cracking location in plate-fin structures is consistent with the peak value of equivalent stress in actual operation process. Therefore, in this paper, the influence of structure parameters are investigated for the peak value of equivalent stress in plate-fin structures in the actual operation process of LNG PFHE.

3. Finite element analysis

3.1. The model description

Plate-fin structures, as the core component of LNG PFHE, mainly consist of fins and plate (Carey and Mandrusiak, 1986; Manglik and Bergles, 1995), as shown in Fig. 1. Due to the cyclical repeatability and complexity of plate-fin structures, some issues need to be simplified in the numerical simulation: (1) the impact of layers number is ignored for the stress of plate-fin structures; (2) the flow of natural gas (NG) and mixture refrigerant (MR) is assumed to be alternating and counterflow, as shown in Fig. 1; (3) both materials are assumed to be isotropic and linear elastic; the material parameters are also assumed to be temperature dependent; (4) both brazing material and base metal are supposed to take an elastic deformation; and (5) in the brazing process, the flow of liquid

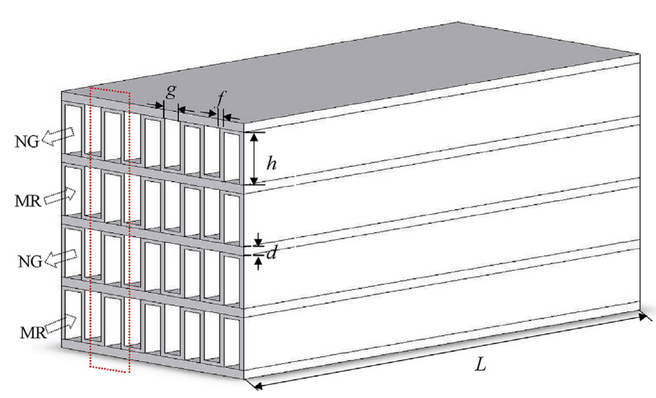

Fig. 1. The diagram of Plate-fin structures (d is Plate Thickness; f, Fin Thickness; h, Fin Height; L, Effective Length; δ, Brazing Seam Thickness; and g, Fin Distance).

brazing material, the diffusion and dissolution of brazing material to base metal, and the capillary reaction of brazing material are ignored. In other words, the brazing plate-fin structures are perfect. In this work, only one unit of plate-fin structures (as dotted lines shown in Fig. 1) which consists of four layers plate and fin, is analyzed because the plate-fin structures are periodic and symmetrical. Meanwhile, a very short length (L) is selected in the unit of plate-fin structures because the change of fluid temperature is very slight in a very short length (L) along the length direction of plate-fin structures. Fig. 2(a) shows the simplified model of plate-fin structures. Fig. 2(b) and (c) display the local structure of region 2 and regions 4, 5 and 6 in Fig. 2(a), respectively. At the same time, the structure parameters of plate-fin structures are also shown in Figs. 1 and 2(a).

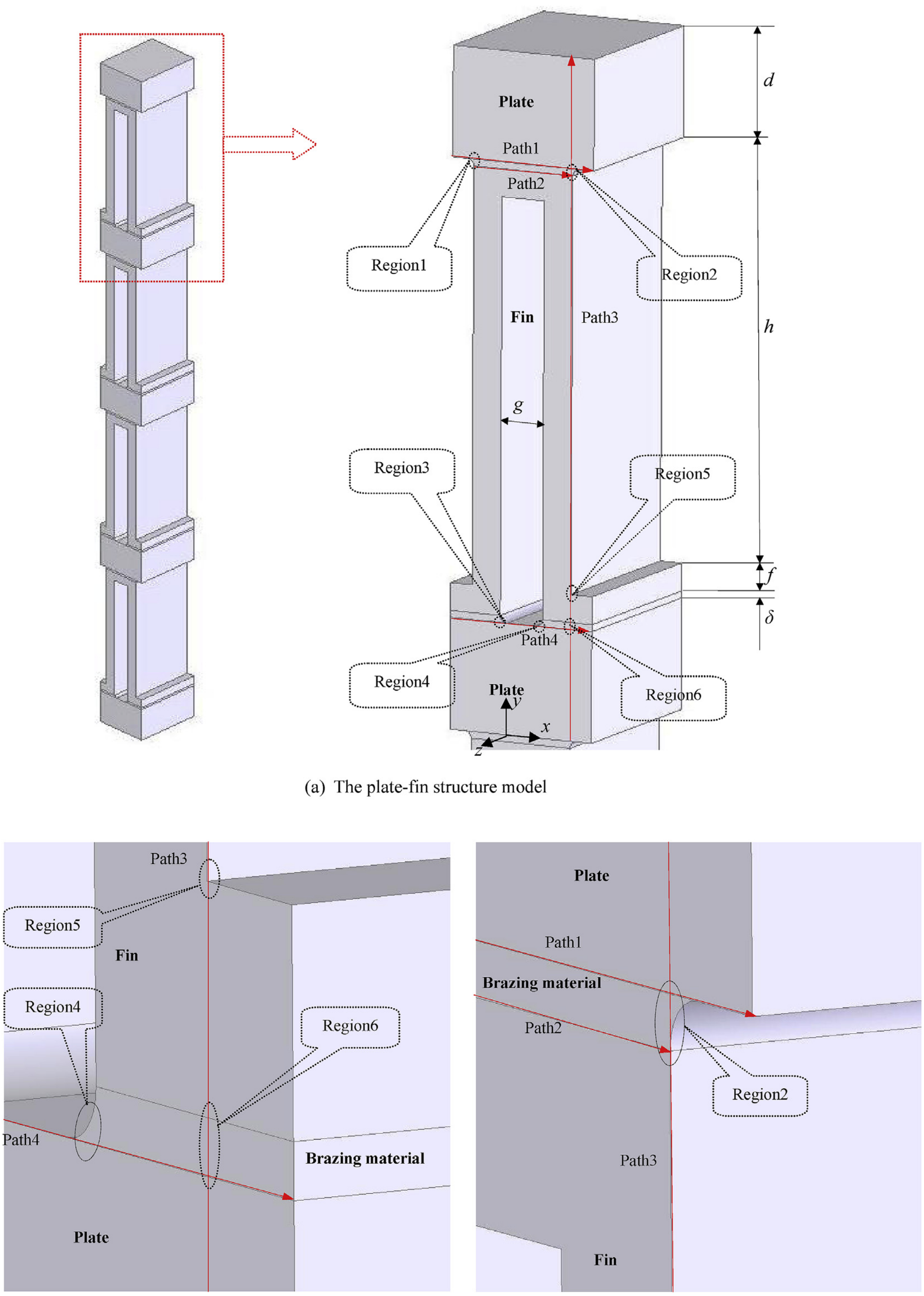

(a) The plate-fin structure model

(b) The local structure of region 2 (c) The local structure of regions 4, 5 and 6

Fig. 2. The simplified plate-fin structure model and local structure.

3.2. Material properties

In this analysis, the fin and plate are assumed to be AL3003 and brazing material is AL4004. In order to get fine results, the expansion coefficient and elastic modulus are assumed to be temperature dependent for the AL3003 and the AL4004. Table 1 lists all the required material properties used in the simulations.

3.3. Analysis strategy

For thermal analysis, the convective heat transfers between NG or MR and the wall of plate-fin structures are applied, because the heat transfer process with phase change between the NG and the MR is implemented by the convective heat transfer between NG or MR and the wall of plate-fin structures and the heat conduction in the plate-fin structures. The convective heat transfer can be expressed as:

$$q = h\left(T_f - T_w\right) \tag{1}$$

where q is heat flux; h is convective heat transfer coefficient; T_w is wall temperature; T_f is the fluid temperature, such as NG or MR.

For the stress analysis, cyclical symmetry boundary on the leftmost and rightmost surfaces is considered due to the periodicity and symmetry of plate-fin structures. The nodes on the bottom surface are constrained in vertical direction. At the same time, the operating pressure of NG and MR is applied to simulate the interaction between NG or MR and the wall of plate-fin structures. The impact of external load is ignored in the investigation on the stress of plate-fin structures because the liquefied heat exchanger can freely expand or shrink by means of the free slide of sliding guide frame under the support structure.

According to the simplified model of plate-fin structures in Fig. 2 and the above boundary condition, the analysis model is established based on finite element method and thermal elastic theory using ANSYS software. At the same time, the more grid numbers there are, the larger number finite control volumes there are. Consequently, it will reduce the computational efficiency. Therefore, the computational domain is discretized into hexahedral finite control volumes so as to decrease the grid numbers and improve the computation efficiency. The mesh-independent is also tested for the model in different structure parameters of LNG PFHE according to the method from the reference (Ma et al., 2016).

At the same time, the interaction between temperature field and strain field needs to be considered because of the relatively large deformation on plate-fin structures in the actual operation process of LNG PFHE. Therefore, the direct coupling method based on thermal elastic theory is used to analyze the stress characteristics of plate-fin structures in LNG PFHE. In the mean time, ANSYS Parametric Design Language is adopted to program the above simulation process, and the above analysis method is also validated by the experimental data in reference (Ma et al., 2014).

According to the reference (Ma et al., 2015), the peak value of equivalent stress in plate-fin structures increases as the temperature of MR increases in actual operation process of LNG PFHE. In other words, the stress of plate-fin structures is larger in the MR entrance of LNG PFHE than that in other regions. Therefore, the stress distributions of plate-fin structures are analyzed and the influence of structure parameters is investigated for the stress of plate-fin structures in the MR entrance of LNG PFHE. For the LNG PFHE in a large-scale LNG cold-box in which the yield is 2.6×10^6 tons in per year, the NG is cooled from 210 K to 150 K and becomes liquid by condensation heat transfer at the NG pressure P_{NG} = 7.1 MPa and the MR is heated from 155 K to 215 K and vaporized by the boiling heat transfer at the MR pressure P_{MR} = 0.4 MPa according to the literature (Ma et al., 2014, 2015). In other words, the temperature of NG and MR are 215 K and 210 K in the MR entrance of LNG PFHE, respectively. At the same time, the stress of plate-fin structures is slightly influenced by the heat exchange performance of LNG PFHE when the temperature difference between NG and MR is no more than 5 K in the actual operation process (Ma et al., 2014, 2015). Therefore, the heat transfer coefficient between NG and the wall of plate-fin structures is assumed to be 1.5 kW/(m^2 K) at the NG temperature T_{NG} = 215 K and the NG pressure P_{NG} = 7.1 MPa; the heat transfer coefficient between MR and the wall of plate-fin structures is assumed to be 1 kW/(m^2 K) at the MR temperature T_{MR} = 210 K and the MR pressure P_{MR} = 0.4 MPa. To sum up, in this paper, the influence of structure parameters is investigated for the stress of plate-fin structures at the heat transfer coefficient h_{NG} = 1.5 kW/(m^2 K), h_{MR} = 1 kW/(m^2 K), the temperature T_{NG} = 215 K, T_{MR} = 210 K and the pressure P_{NG} = 7.1 MPa, P_{MR} = 0.4 MPa.

4. Results and discussion

4.1. Stress distribution

In this section, the stress distributions of plate-fin structures are analyzed in a very short length near the MR entrance of the liquefied heat exchanger in actual operation process. In order to better understand the stress distribution of plate-fin structures, four reference paths are selected, as marked in Fig. 2. Figs. 3–7 present the stress distributions of four reference paths in plate-fin structures. The plots are drawn based on the parameter setting in section 3.3. Figs. 3 and 4 are the stress distributions of paths 1 and 2, respectively (σ_x, σ_y and σ_z are direct stress along x, y and z directions, respectively; τ_{xy} and τ_{yz} are shear stress on x-y plane and y-z plane, respectively). Path 1 and 2 are located at the interface between the brazing filler metal and the plate and between the brazing filler metal and the fin, respectively. The results show that the three direct stresses and the equivalent stress are

Table 1
Material parameters used in FEM simulation.

Material	Temperature, K	E, GPa	CET (10^{-6}), 1/K	Poisson's ratio	Specific heat, J/(kg K)	Density, kg/m^3	Conductivity, W/(m K)
AL3003	305	68.9	22.4	0.33	962	2740	159
	250	70.6	19.7				
	195	72.4	16.9				
	175	73.2	15.9				
	145	74.5	14.4				
AL4004	305	94.6	15.1	0.35	864	2710	155
	250	96.4	14.9				
	195	98.2	14.7				
	175	98.8	14.6				
	145	99.6	14.5				

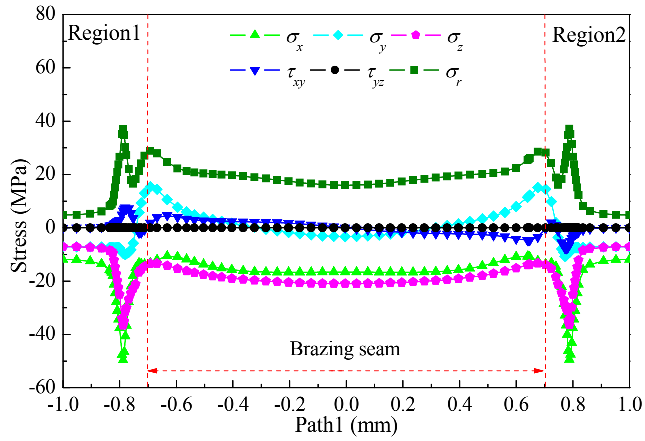

Fig. 3. Stress distribution of path 1.

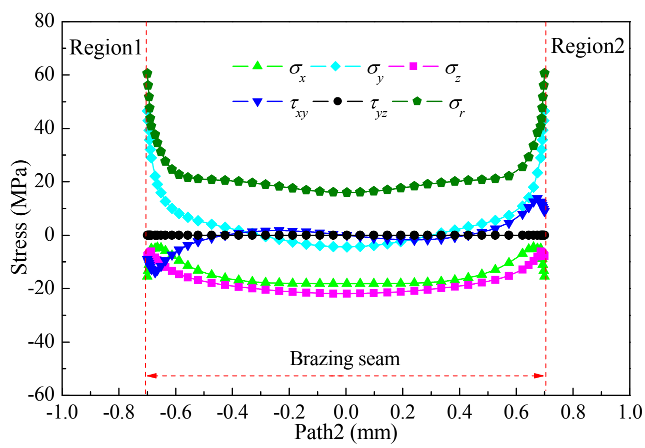

Fig. 4. Stress distribution of path 2.

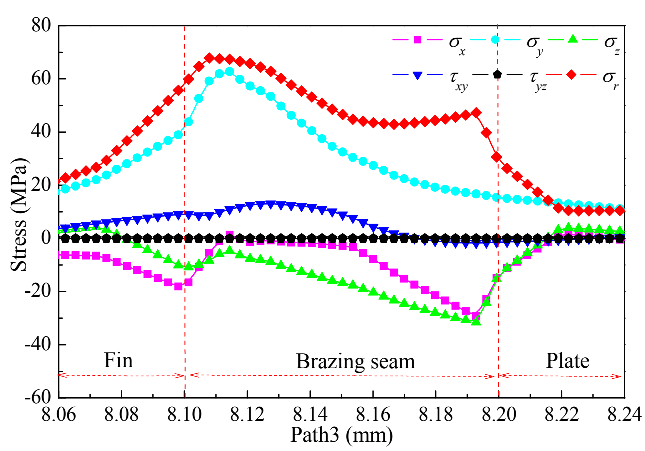

Fig. 5. Stress distribution of the local position in region 2.

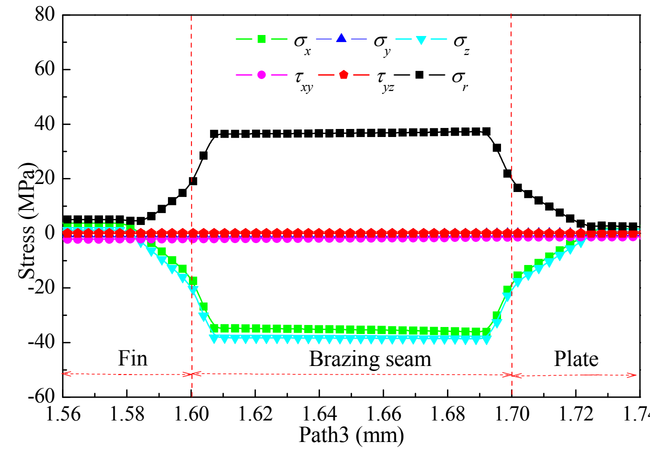

Fig. 6. Stress distribution of the local position in region 6.

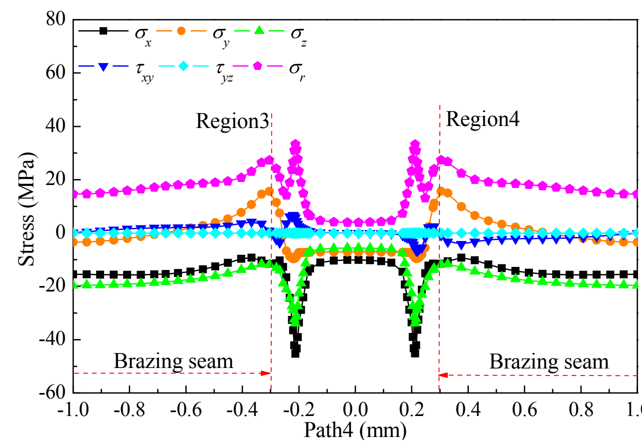

Fig. 7. Stress distribution of path 4.

symmetrically distributed while the shear stresses are unsymmetrical. The stress gradient is much larger at the brazed joint (regions 1 and 2) which is a small transitional arc on the two terminals of the brazing seam than that at the adjacent region in actual operation process of LNG PFHE in a large-scale LNG cold-box.

From Fig. 3, it can be also seen clearly that the direct stresses in *x* and *z* directions and the equivalent stress will reach the peak value at the brazed joint. The equivalent stress, the direct stress in *y* direction and the shear stress on *x*-*y* plane are complex at brazed joint near plate side in actual operation process of LNG PFHE. At the same time, the direct stresses in *x* and *z* directions are prominent while the shear stresses on *x*-*y* plane and *y*-*z* plane and the direct stress in *y* direction are relatively small at the brazed joint and brazing seam layer near plate side. Hence, the direct stresses in *x* and *z* directions are the major factors to influence the strength of the brazed joint and brazing seam layer near plate side in the MR entrance of LNG PFHE.

Fig. 4 shows that the direct stress in *y* direction and the equivalent stress will reach the peak value at the brazed joint. The direct stress in *y* direction is prominent while the direct stresses in *x* and *z* directions and the shear stresses are relatively small at brazed joint near fin side. At the same time, the direct stresses in *x* and *z* directions are also prominent at brazing seam layer near fin side in the MR entrance of LNG PFHE. Therefore, the direct stress in *y* direction is the main factor to influence the strength of plate-fin structures at brazed joint near fin side while the direct stresses in *x* and *z* directions are the main factors to influence that at brazing seam layer near fin side in the MR entrance of LNG PFHE.

According to the above analysis, the stresses are complex and reach peak value at the brazed joint of plate-fin structures in the MR entrance of LNG PFHE. In order to further analyze stresses at the brazed joint of plate-fin structures in the MR entrance of LNG PFHE, the stress distributions of the local position in region 2 are given in

Fig. 5. The results illustrate that the equivalent stress at brazed joint near the fin side is larger than that near the plate side. At the same time, the direct stress in y direction is prominent at brazed joint near fin side while the direct stresses in x and z directions are prominent in brazed joint near plate side in the MR entrance of LNG PFHE. These results are consistent with that from Figs. 3 and 4.

Fig. 6 depicts the stress distribution of the local position in region 6. The results show that the direct stresses in x and z directions and the equivalent stress also reach the peak value at brazing seam layer while the shear stresses on x-y plane and y-z plane and the direct stress in y direction are relatively small at that layer. In other words, the direct stresses in x and z directions are main factors to influence the strength of the brazing seam layer for plate-fin structures in the MR entrance of LNG PFHE.

Fig. 7 exhibits the stress distribution of path 4. These results are also obtained that the stress gradient is much larger at the brazed joint (regions 3 and 4). And the direct stresses in x and z direction are prominent while the shear stresses on x-y plane and y-z plane are relatively small.

To sum up, the stresses are complex at the brazed joints of plate-fin structures in actual operation process of LNG PFHE. The equivalent stress at brazed joint near the fin side is larger than that in other regions. The direct stress in y direction is prominent at brazed joint near fin side. The structural strength of plate-fin structures is directly impacted by the stress at brazed joint near fin side due to the influence of direct stress in y direction.

4.2. *The influence of structure parameters for stress*

In section 4.1, it is stated that the equivalent stress will reach to the peak value in the brazed joint of plate-fin structures. If the design is unreasonable for the structure parameters of LNG PFHE, it is likely to induce a crack failure in these regions. So it is necessary to study the influence of structure parameters on the stress of plate-fin structures. In the following contents, the influence of structure parameters will be analyzed on the stress of plate-fin structures in actual operation process of LNG PFHE in a large-scale LNG cold-box.

4.2.1. *The influence of fin height*

Fig. 8 is the relation between the peak value of equivalent stress and fin height at different fin thickness for fin distance $g = 0.6$ mm, brazing seam thickness $\delta = 0.1$ mm and plate thickness $d = 1.6$ mm. The results show that the peak value of equivalent stress increases as the fin height increases. But there is a slight influence of fin height on the peak value of equivalent stress of plate-fin structures in the MR entrance of LNG PFHE. Fig. 9 depicts the relation between the peak value of equivalent stress and fin height at different fin distance for fin thickness $f = 0.4$ mm, brazing seam thickness $\delta = 0.1$ mm and plate thickness $d = 1.6$ mm. The results are similar to the previous parameter settings. To sum up, for plate-fin structures in the MR entrance of LNG PFHE, the peak value of equivalent stress increases with the increase of fin height and is slightly impacted by that. Therefore, the structural strength of plate-fin structures is slightly influenced by the fin height. In the actual engineering, it is unnecessary to consider the influence of fin height on the structural strength of plate-fin structures in LNG PFHE.

4.2.2. *The influence of plate thickness*

Figs. 10 and 11 present the relation between the peak value of equivalent stress and plate thickness. Fig. 10 is the relation between the peak value of equivalent stress and plate thickness at different fin distance for fin thickness $f = 0.4$ mm, brazing seam thickness $\delta = 0.1$ mm and fin height $h = 6.0$ mm. Fig. 11 is the relation between the peak value of equivalent stress and plate thickness at different fin thickness for fin distance $g = 0.6$ mm, brazing seam thickness $\delta = 0.1$ mm and fin height $h = 6.0$ mm. The results indicate that the peak value of equivalent stress decreases as the plate thickness increases and is slightly impacted by the plate thickness. At the same time, the larger fin distance or the smaller fin thickness is, the lager peak value of equivalent stress is. For plate-fin structures in LNG PFHE, the manufacturing cost and materials will increase with the increase of plate thickness. According to the above results, the influence of plate thickness is slight on the structural strength of plate-fin structures in LNG PFHE. Therefore, in order to reduce manufacturing cost and save manufacturing materials in actual engineering, it is necessary to decrease the plate thickness when the brazed quality can be met.

4.2.3. *The influence of brazing seam thickness*

Fig. 12 depicts the relation between the peak value of equivalent stress and brazing seam thickness at different fin thickness for fin distance $g = 0.6$ mm, fin height $h = 6.0$ mm and plate thickness $d = 1.6$ mm. The results show that the peak value of equivalent stress decreases with the increase of brazing seam thickness. The thicker the fin is, the smaller the peak value of equivalent stress is. At the same time, the peak value of equivalent stress is obviously impacted by the brazing seam thickness. Fig. 13 presents the relation between the peak value of equivalent stress and brazing seam thickness at different fin distance for fin thickness $f = 0.4$ mm, fin

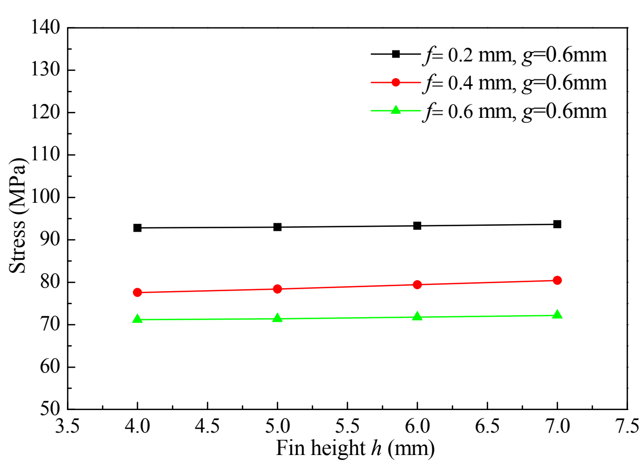

Fig. 8. The peak value of equivalent stress vs. fin height at different fin thickness.

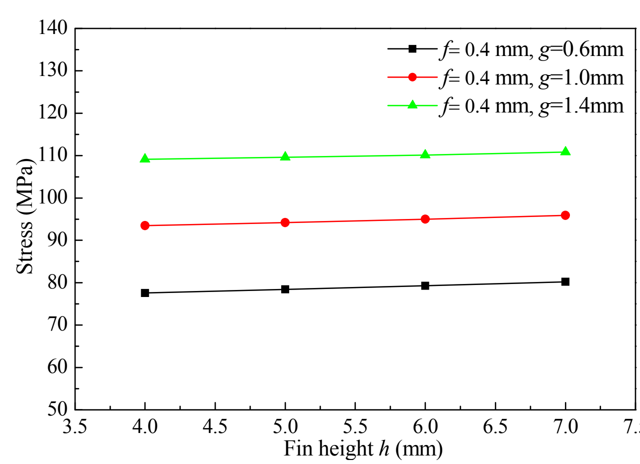

Fig. 9. The peak value of equivalent stress vs. fin height at different fin distance.

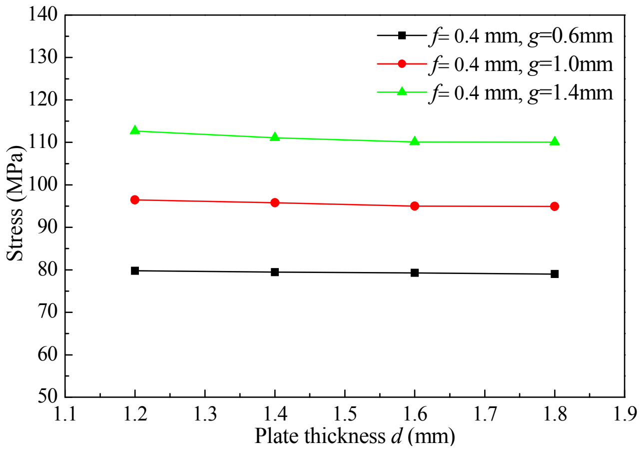

Fig. 10. The peak value of equivalent stress vs. plate thickness at different fin distance.

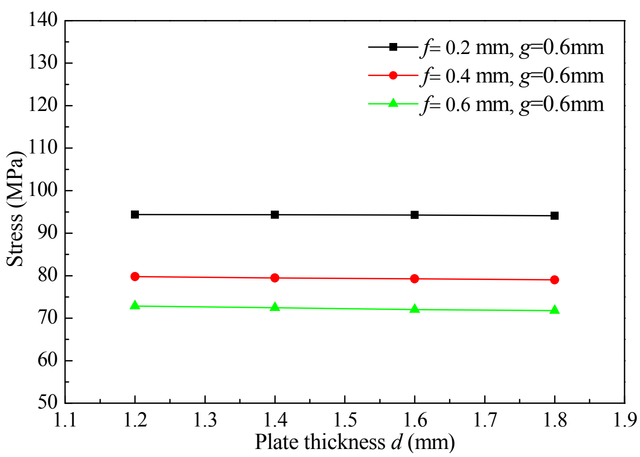

Fig. 11. The peak value of equivalent stress vs. plate thickness at different fin thickness.

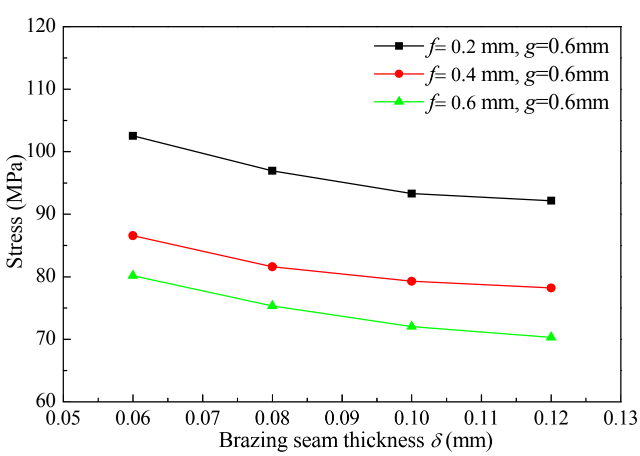

Fig. 12. The peak value of equivalent stress vs. brazing seam thickness at different fin thickness.

height $h = 6.0$ mm and plate thickness $d = 1.6$ mm. The results also indicate that the peak value of equivalent stress decreases with the increase of brazing seam thickness and is obviously impacted by the brazing seam thickness. At the same time, the larger the fin distance is, the larger the peak value of equivalent stress is. The

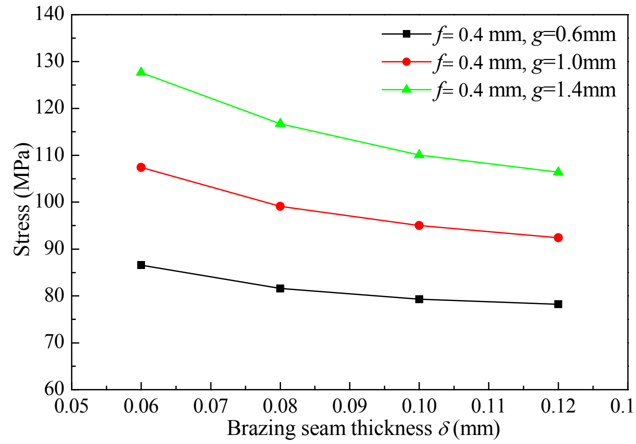

Fig. 13. The peak value of equivalent stress vs. brazing seam thickness at different fin distance.

influence of fin distance is more obvious on the peak value of equivalent stress when the brazing seam thickness is thinner. To sum up, the larger the fin distance or the smaller the fin thickness is, the larger the peak value of equivalent stress is. The influence of brazing seam thickness is obvious on the structural strength of plate-fin structures in LNG PFHE.

According to the above analysis, the peak value of equivalent stress is obviously impacted by the brazing seam thickness and decreases with the increase of brazing seam thickness. In order to further analyze the influence of brazing seam thickness on the stress of plate-fin structures in LNG PFHE, the stress distributions of reference paths are given from Fig. 2 in this paper. Figs. 14–17 are the stress distributions of reference paths at different brazing seam thickness for fin thickness $f = 0.4$ mm, fin height $h = 6.0$ mm, plate thickness $d = 1.6$ mm and fin distance $g = 0.6$ mm. Fig. 14 is the distributions of equivalent stress along path 1 at different brazing seam thickness. The results indicate that the equivalent stress at the brazed joint (regions 1 and 2) near plate side is obviously impacted by the brazing seam thickness and the peak value of that increases as the brazing seam thickness increases. At the same time, the equivalent stress at brazing seam layer (-0.55 mm $< x <$ 0.55 mm) near plate side decreases with the increase of brazing seam thickness. Fig. 15 depicts the stress distributions in different directions along path 1 at different brazing seam thickness. The results show

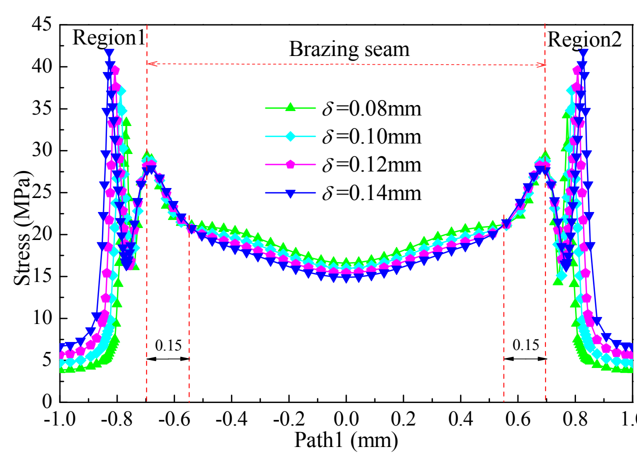

Fig. 14. The distribution of equivalent stress along path 1 at different brazing seam thickness.

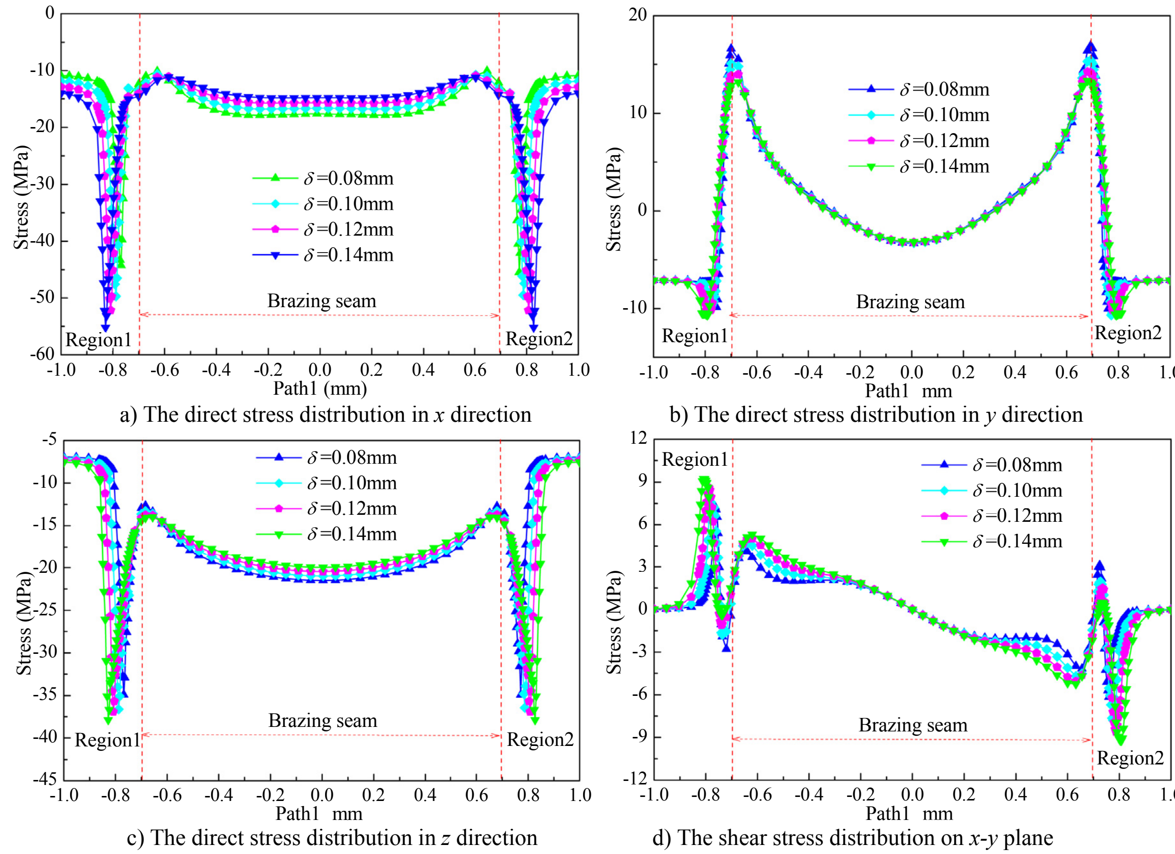

Fig. 15. The stress distribution in different directions along path 1 at different brazing seam thickness.

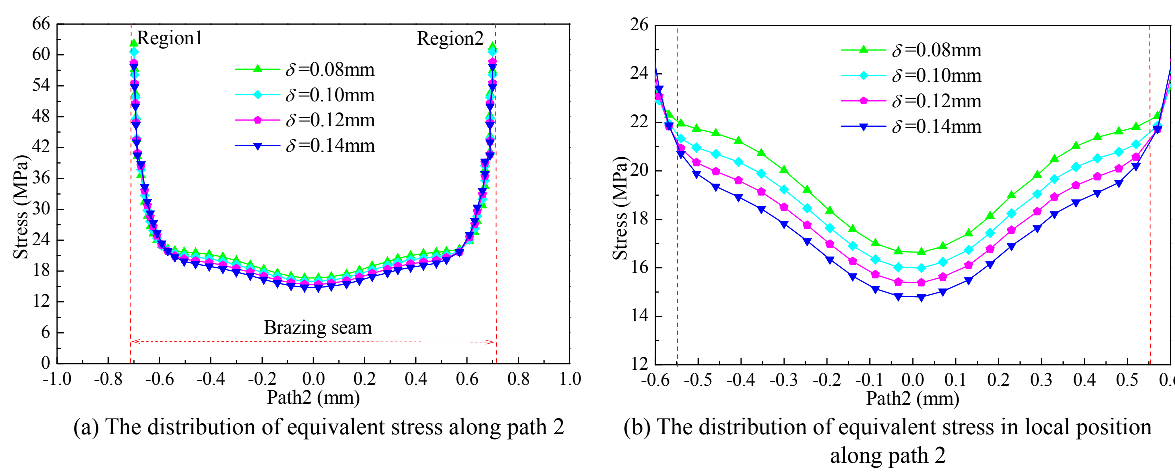

Fig. 16. The distribution of equivalent stress along path 2 at different brazing seam thickness.

that the direct stresses in *x* and *z* directions and the shear stress on *x*-*y* plane at brazed joint (regions 1 and 2) near plate side is obviously impacted by the brazing seam thickness and the peak value of that increases with the increase of the brazing seam thickness. At brazing seam layer near plate side, the direct stresses in *x* and *z* directions decrease with the increase of brazing seam thickness. Therefore, the conclusion can be further obtained that the direct stresses in *x* and *z* directions and the shear stress on *x*-*y* plane are the main factors to induce the increase of the peak value of equivalent stress with the increase of brazing seam thickness at brazed joint (regions 1 and 2) near plate side. The direct stresses in *x* and *z* directions are the main factors to induce the increase of that with the decrease of brazing seam thickness at brazing seam layer near plate side. However, the stresses of path 1 are not the main factors which result in the decline of the peak value of equivalent stress in plate-fin structures with the increase of the brazing seam thickness in LNG PFHE.

Fig. 16 illustrates the distributions of equivalent stress along path 2 at different brazing seam thickness. Fig. 16(b) is partial enlargement for Fig. 16(a). The results show that the equivalent

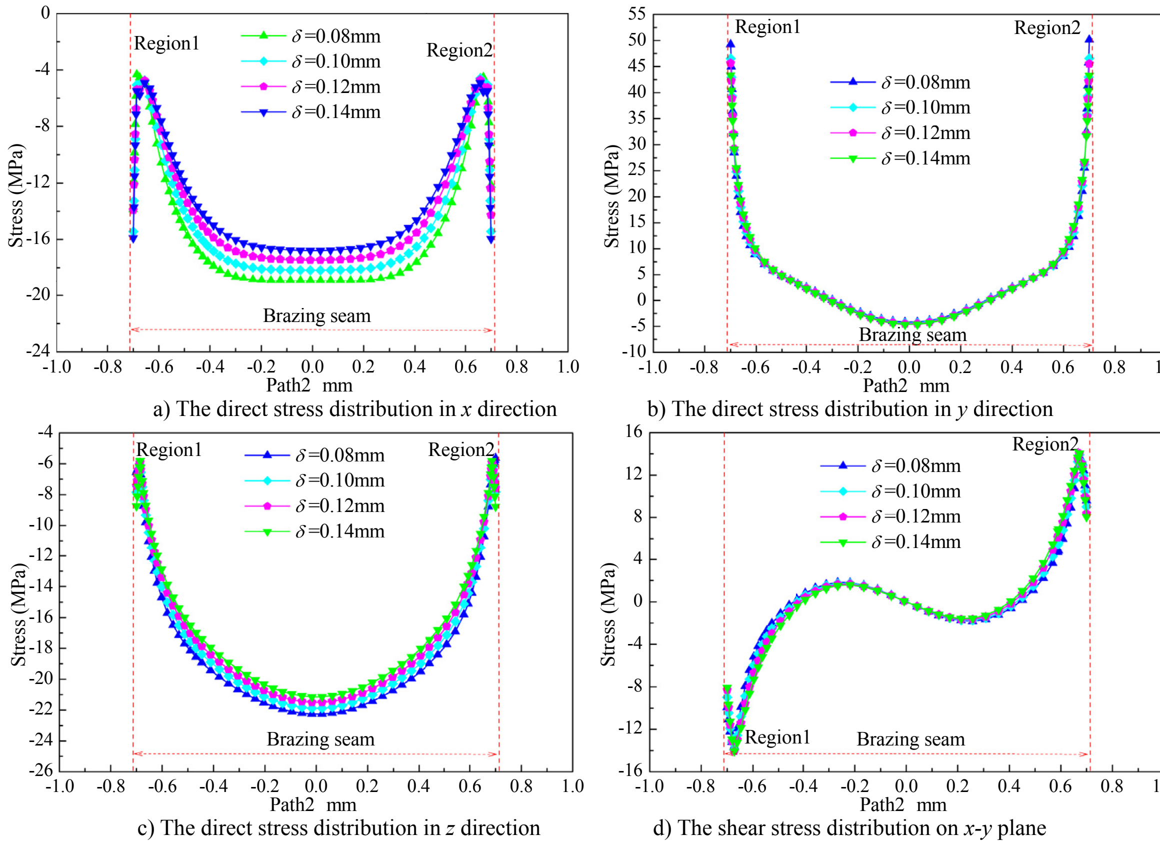

Fig. 17. The stress distribution in different directions along path 2 at different brazing seam thickness.

stress at the brazed joint (regions 1 and 2) and the brazing seam layer (-0.55 mm $< x <$ 0.55 mm) near fin side increases as the brazing seam thickness decreases. According to the analysis from the section 4.1, the equivalent stress will reach the peak value at the brazed joint of plate-fin structures and the equivalent stress at brazed joint near the fin side is much larger than that near the plate side. Therefore, the influence of brazing seam thickness on the equivalent stress at brazed joint near the fin side are main reasons which result in the decline of the peak value of equivalent stress decreases with the increase of brazing seam thickness. Similarly, the stress distributions in different directions along path 2 are also given in Fig. 17. The results show that the direct stress in *y* direction at the brazed joint near the fin side decreases with the increase of brazing seam thickness. The brazing seam thickness has more obvious influence on the direct stress in *y* direction than that in other directions at brazed joint near the fin side. At the brazing seam layer near fin side, the direct stresses in *x* and *z* directions decrease as the brazing seam thickness increases and is obviously impacted by that. In other words, the direct stress in *y* direction is the main factor to induce the decrease of equivalent stress with the increase of brazing seam thickness at brazed joint (regions 1 and 2) near fin side. The direct stresses in *x* and *z* directions are main reasons to induce the decrease of that with the increase of brazing

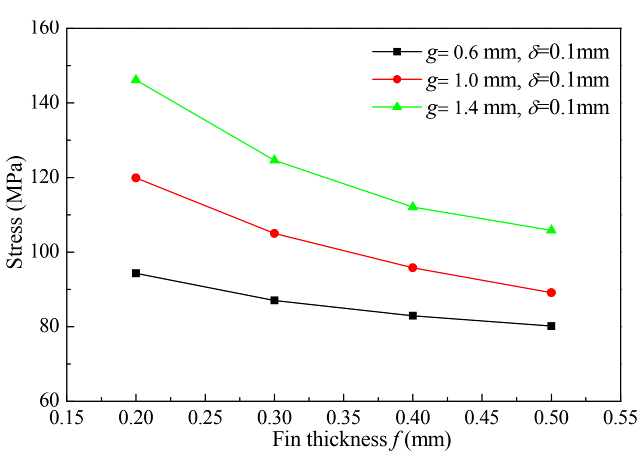

Fig. 18. The peak value of equivalent stress vs. fin thickness at different fin distance.

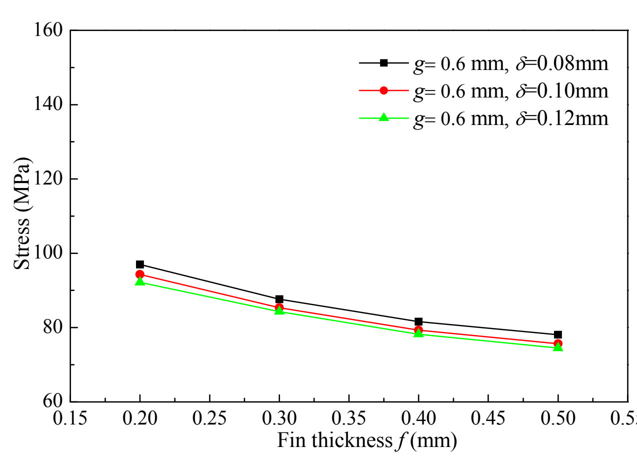

Fig. 19. The peak value of equivalent stress vs. fin thickness at different brazing seam thickness.

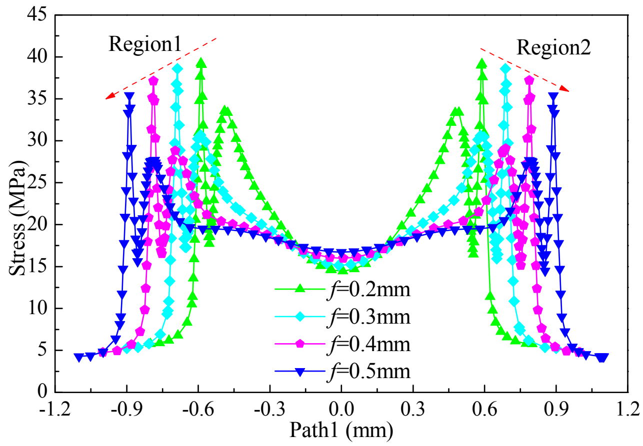

Fig. 20. The distribution of equivalent stress along path 1 at different fin thickness.

seam thickness at brazing seam layer near fin side. At the same time, the influence of brazing seam thickness on the peak value of equivalent stress in plate-fin structures is mainly induced by the direct stress in *y* direction at the brazed joint (regions 1 and 2) near fin side.

To sum up, the structural strength of plate-fin structures in LNG PFHE is obviously impacted by the brazing seam thickness and the direct stress in *y* direction is main reason to cause the above results at brazed joint (regions 1 and 2) near fin side. At the same time, the influence of brazing seam thickness on the structural strength of plate-fin structures at brazed joint near plate side is induced by the influence of that on the direct stresses in *x* and *z* directions and the shear stress on *x*-*y* plane. At the brazed joint near fin side, that will be induced by the influence of brazing seam thickness on the stress in *y* direction.

4.2.4. The influence of fin thickness

Figs. 18 and 19 show the relation between the peak value of equivalent stress and fin thickness. Fig. 18 presents the relation between the peak value of equivalent stress and fin thickness at different fin distance for plate thickness $d = 1.6$ mm, brazing seam thickness $\delta = 0.1$ mm and fin height $h = 6.0$ mm. Fig. 19 is the relation between the peak value of equivalent stress and fin thickness at different brazing seam thickness for fin distance $g = 0.6$ mm, fin thickness $f = 0.4$ mm and fin height $h = 6.0$ mm. The results indicate that the peak value of equivalent stress decreases as the fin thickness increases and is obviously impacted by that. At the same time, the influence of fin distance on the peak value of equivalent stress is more obvious when the fin thickness is smaller. In other words, it is necessary to increase the fin thickness in order to improve the structural strength of plate-fin structures in LNG PFHE.

In order to further analyze the influence of fin thickness on the stress of plate-fin structures in LNG PFHE, the stress distributions of reference paths from Fig. 2 are also given at different fin thickness. Figs. 20–23 are the stress distributions of reference paths at different fin thickness for brazing seam thickness $\delta = 0.1$ mm, fin height $h = 6.0$ mm, plate thickness $d = 1.6$ mm and fin distance $g = 0.6$ mm. Fig. 20 is the distributions of equivalent stress along path 1 at different fin thickness. The results show that the peak

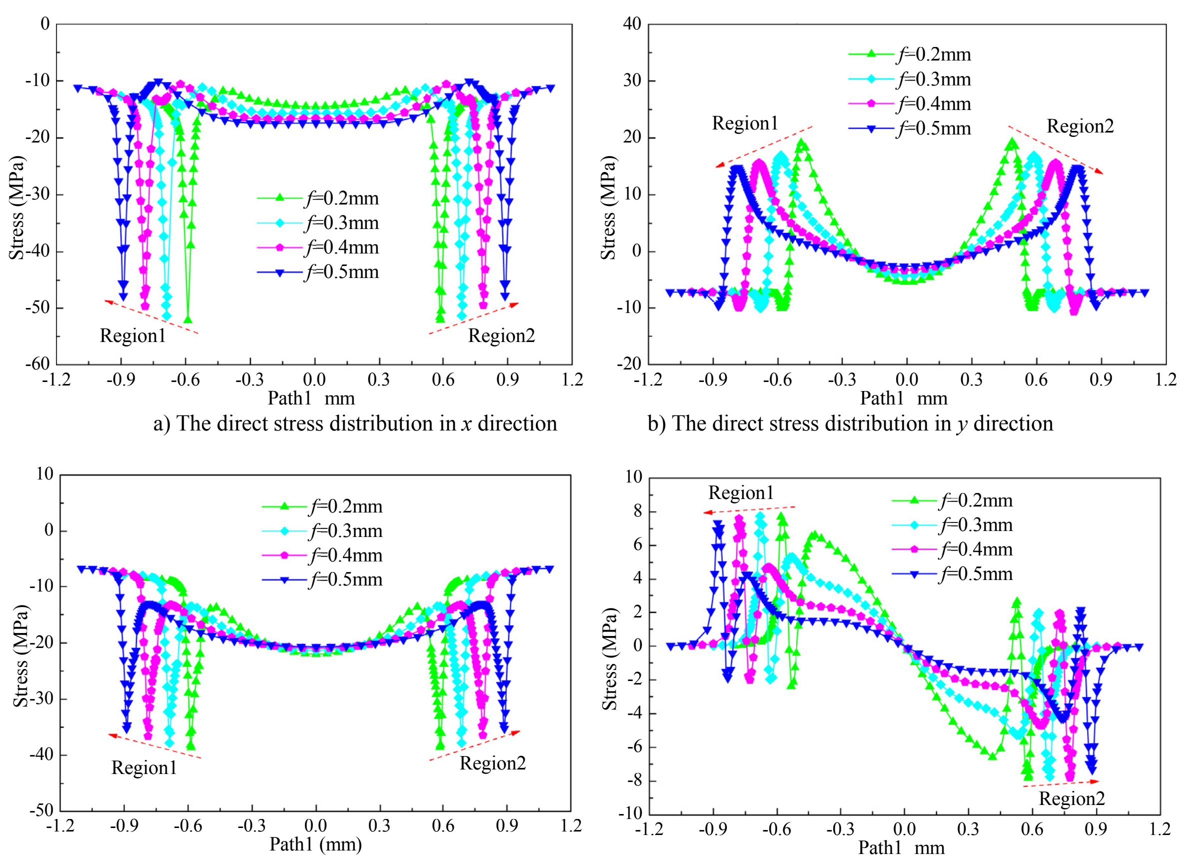

a) The direct stress distribution in *x* direction
b) The direct stress distribution in *y* direction
c) The direct stress distribution in *z* direction
d) The shear stress distribution on *x*-*y* plane

Fig. 21. The stress distribution in different directions along path 1 at different fin thickness.

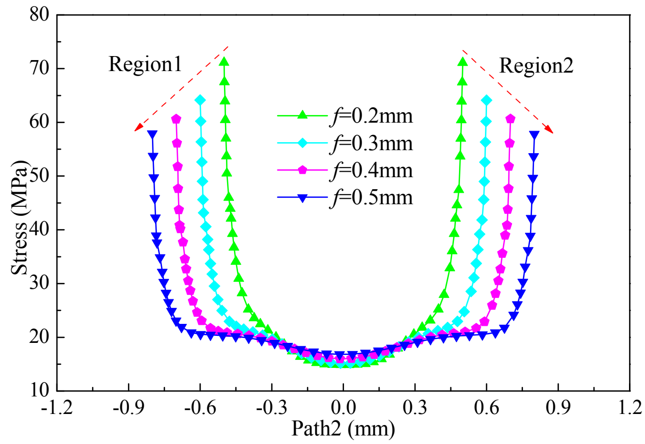

Fig. 22. The distribution of equivalent stress along path 2 at different fin thickness.

value of equivalent stress decreases with the increase of fin thickness at the brazed joint near plate side. And the equivalent stress is obviously impacted by the fin thickness at brazed joint near plate side. Fig. 21 depicts the stress distributions in different directions along path 1 at different fin thickness. The results indicate that the direct stresses in three directions are obviously impacted by the fin thickness at brazed joint near plate side and the peak value of that decreases as the fin thickness increases. At the same time, the direct stress in *x* direction increases with the increase of fin thickness at brazing seam layer near plate side and the influence of fin thickness is more obvious on the direct stress in *x* direction than that on the stresses in other directions. In other words, the influence of fin thickness on the peak value of equivalent stress at brazed joint near plate side is mainly induced by the direct stresses in three directions while that at brazing seam layer near plate side is mainly induced by the direct stress in *x* direction.

Fig. 22 depicts the distributions of equivalent stress along path 2 at different fin thickness. The results show that the equivalent stress will also reach the peak value at brazed joint near fin side. The peak value of equivalent stress decreases with the increase of fin thickness at brazed joint near fin side and is also obviously impacted by the fin thickness. But the equivalent stress is slightly impacted by that at brazing seam layer near fin side. In order to further analyze the stress distributions of path 2 at different fin thickness, the stress distributions in different directions along path 2 at different fin thickness are given in Fig. 23. The results indicate that the peak value of direct stresses in three directions at brazed joint near fin side decreases as the fin thickness increases. But the influence of fin thickness on the peak value of direct stress in *y* direction is more obvious than that in other directions. The shear stress on *x*-*y* plane is slightly impacted by the fin thickness at brazed joint near fin side. In other words, the influence of fin thickness on the peak value of equivalent stress at brazed joint near fin side is mainly induced by the direct stress in *y* direction.

In short, the structural strength of plate-fin structures is obviously influenced by the fin thickness in actual operation process of LNG PFHE and the peak value of equivalent stress decreases with the increase of fin thickness. In other words, the increasing fin thickness is an effective measure to improve the structural strength of plate-fin structures in LNG PFHE. At the same time, the direct

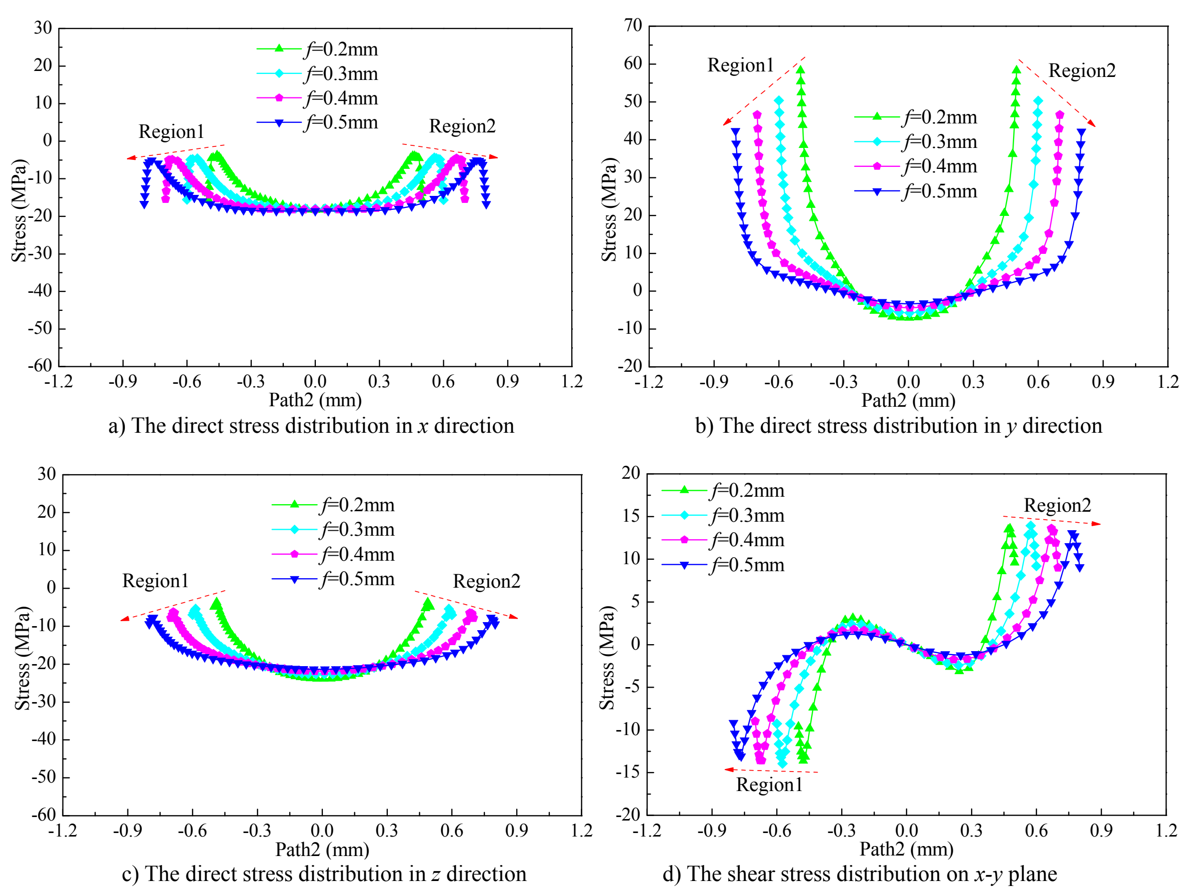

Fig. 23. The stress distribution in different directions along path 2 at different fin thickness.

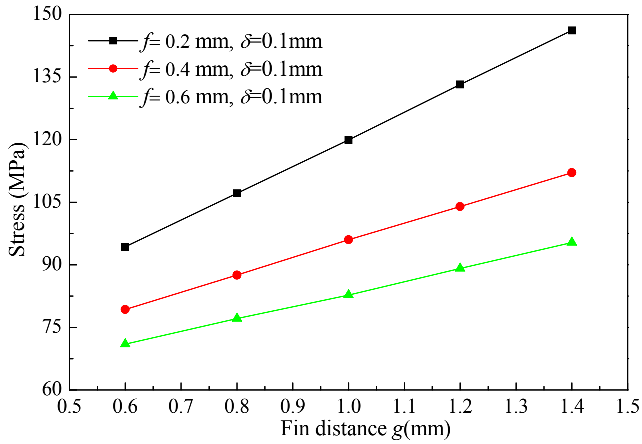

Fig. 24. The peak value of equivalent stress vs. fin distance at different fin thickness.

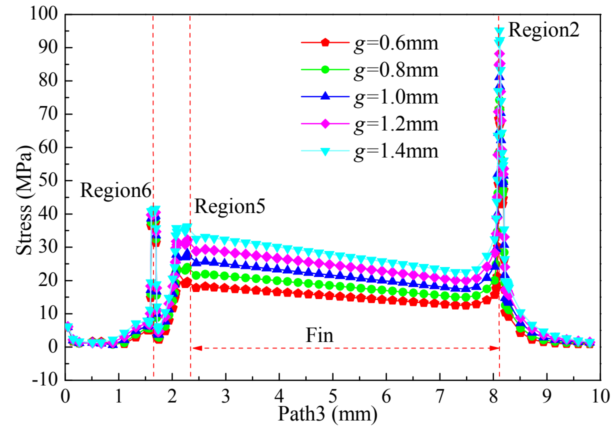

Fig. 26. The distribution of equivalent stress along path 3 at different fin distance.

stresses in three directions are main factors that cause the structural strength of plate-fin structures at brazed joint near plate side obviously being impacted by the fin thickness. However, at the brazed joint near fin side in LNG PFHE, the direct stress in *y* direction will result in that the structural strength of plate-fin structures decreases with the increase of fin thickness.

4.2.5. The influence of fin distance

Figs. 24 and 25 are the relation between the peak value of equivalent stress and fin distance. Fig. 24 presents the relation between the peak value of equivalent stress and fin distance at different fin thickness for plate thickness $d = 1.6$ mm, brazing seam thickness $\delta = 0.1$ mm and fin height $h = 6.0$ mm. Fig. 25 is the relation between the peak value of equivalent stress and fin distance at different brazing seam thickness for plate thickness $d = 1.6$ mm, fin thickness $f = 0.4$ mm and fin height $h = 6.0$ mm. The results show that the peak value of equivalent stress increases linearly with the increase of fin distance and is obviously impacted by that. At the same time, the larger fin distance is, the more obvious influence of brazing seam thickness and fin thickness is. In other words, the structural strength of plate-fin structures is obviously impacted by the fin distance and can be improved by the decreasing fin distance.

For the sake of analyzing the influence of fin distance on the structural strength of plate-fin structures in LNG PFHE, the stress distributions of reference paths from Fig. 2 are also given at different fin distance. Figs. 26–30 are the stress distributions of reference paths at different fin distance for brazing seam thickness $\delta = 0.1$ mm, fin height $h = 6.0$ mm, plate thickness $d = 1.6$ mm and fin thickness $f = 0.4$ mm. Fig. 26 is the distributions of equivalent stress along path 3 at different fin distance. The results show that the equivalent stress is complex at the brazed joint (region 2), brazing seam layer (region 6), and sudden-change location of fin-plate structures (region 5) and will reach the peak value at these positions. At the same time, the equivalent stress along fin height increases with the increase of fin distance and is obviously impacted by that.

In order to further analyze the stress distributions of the local position in region 2 and 6, the distributions of equivalent stress are also given in region 2 and 6. Fig. 27 is the distributions of equivalent stress in region 6 at different fin distance. The results indicate that the equivalent stress at the brazing seam layer is obviously impacted by fin distance and increases as the fin distance increases. At the same time, the equivalent stress at brazing seam layer is larger than that at adjacent region. Fig. 28 is the stress distributions of region 6 in different directions at different fin distance. The results show that the direct stress in *y* direction increases as the fin distance increases. At the same time, the direct stress in *y* direction is obviously impacted by the fin distance at brazing seam layer while the direct stresses in *x* and *z* directions and the shear stress

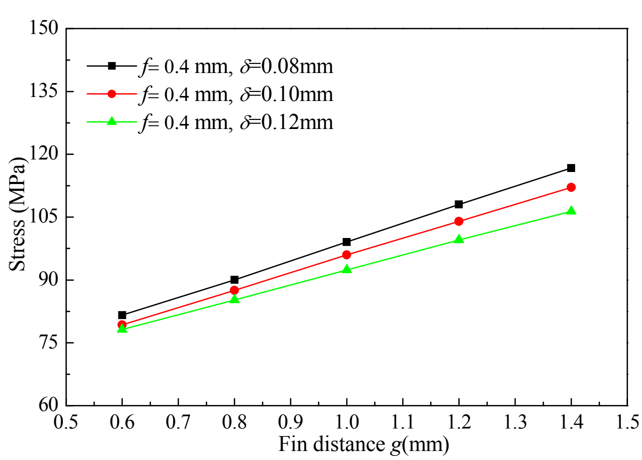

Fig. 25. The peak value of equivalent stress vs. fin distance at different brazing seam thickness.

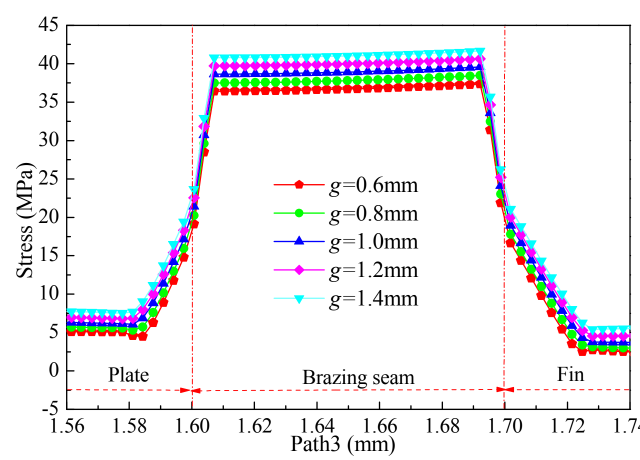

Fig. 27. The equivalent stress distribution of the local position in region 6 at different fin distance.

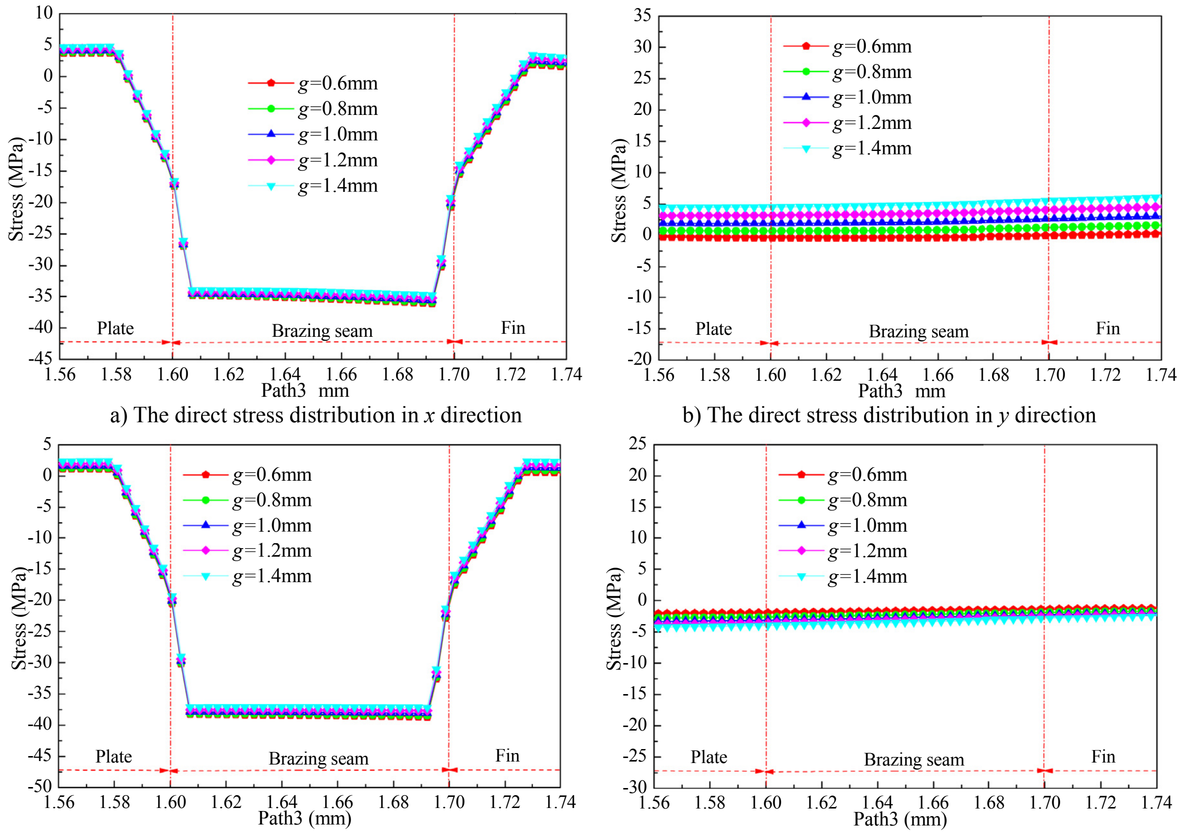

a) The direct stress distribution in x direction

b) The direct stress distribution in y direction

c) The direct stress distribution in z direction

d) The shear stress distribution on x-y plane

Fig. 28. The stress distribution of region 6 in different directions at different fin distance.

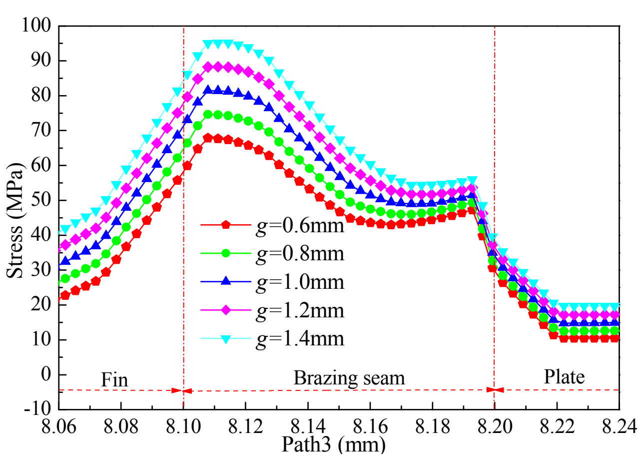

Fig. 29. The equivalent stress distribution of the local position in region 2 at different fin distance.

on x-y plane are slightly impacted by that. This further indicates that the increase of equivalent stress with the fin thickness is induced by the direct stress in y direction at brazing seam layer.

Fig. 29 is the distributions of equivalent stress in region 2 at different fin distance. The results show that the equivalent stress increases with the increase of fin distance at brazed joint and is obviously impacted by fin distance. At the same time, the equivalent stress near fin side is larger than that near plate side. In other words, the peak value of equivalent stress increases with the increase of fin distance because of the influence of fin distance on the equivalent stress near fin side. Fig. 30 illustrates the stress distributions of region 2 in different directions at different fin distance. The results indicate that the direct stress in y direction is obviously impacted by the fin distance and increases with the increase of fin distance. The direct stresses near plate side in x and z directions decrease with the increase of fin distance. At the same time, the direct stresses in x and z directions and the shear stress on x-y plane are slightly impacted by the fin distance. In other words, the influence of fin distance on the peak value of equivalent stress in fin-plate structures is induced by the direct stress near fin side in y direction and the peak value of equivalent stress increases with the increase of fin distance because the direct stress near plate side in y direction increases with the increase of fin distance.

To sum up, the structural strength of plate-fin structures is obviously influenced by the fin distance and the peak value of equivalent stress increases linearly with the increase of fin distance. Therefore, the decreasing fin distance is also a method to improve the structural strength of plate-fin structures in LNG PFHE. At the same time, the influence of fin distance on the structural strength of plate-fin structures is mainly induced by the direct stress in y direction.

5. Conclusions

In this paper, the stress distributions of four reference paths in plate-fin structures were obtained from simulation results. The influence of structure parameters on the stress of plate-fin structures in the MR entrance of LNG PFHE was analyzed by means of a direct thermal-stress coupling method based on the thermal elastic

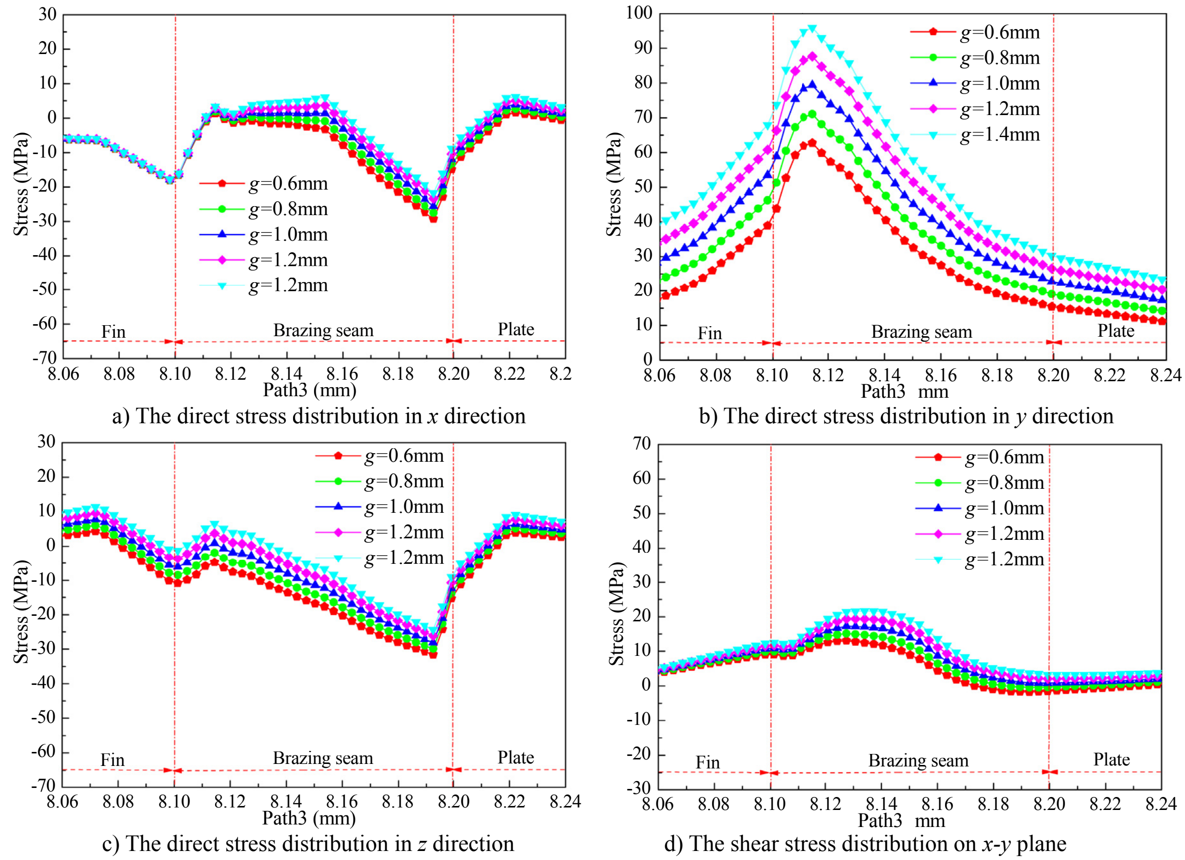

Fig. 30. The stress distribution of region 2 at in different directions at different fin distance.

theory. The some conclusions can be drawn from this investigation.

(1) The stress gradient at the brazed joints is much larger than that at the adjacent regions in actual operation process of LNG PFHE. The structural strength of plate-fin structures is impacted directly by the stress at brazed joint near fin side. At the same time, the direct stress at brazed joint near fin side in *y* direction is a main factor to influence the structural strength of plate-fin structures in LNG PFHE.
(2) The influences of brazing seam thickness, fin thickness and fin distance are obvious on the structural strength of plate-fin structures in actual operation process of LNG PFHE. The direct stress at brazed joint (regions 1 and 2) near fin side in *y* direction is a direct reason which results in the peak value of equivalent stress in plate-fin structures of LNG PFHE increasing with the increase of fin distance and the decrease of brazing seam thickness and fin thickness. In order to improve the structural strength of plate-fin structures in LNG PFHE, it is necessary to increase the brazing seam and fin thickness and decrease the fin distance.
(3) The structural strength of plate-fin structures is slightly impacted by the fin height and plate thickness for the fin height $f = 4.0–7.0$ mm and plate thickness $d = 1.2–1.8$ mm, respectively. Therefore, in order to reduce manufacturing cost and save manufacturing materials, it is necessary to decrease the plate thickness when the brazed quality can be met. At the same time, in the design on the fin height of LNG PFHE, it is unnecessary to consider the influence of fin height on the structural strength of plate-fin structures.

References

Aiyangar, A.K., Neuberger, B.W., Oberson, P.G., Ankem, S., 2005. The effects of stress level and grain size on the ambient temperature creep deformation behavior of an alpha Ti-1.6 wt pct V alloy. Metall. Mater. Trans. A Phys. Metall. Mater. Sci. 36A (3), 637–644.
Brown, T.B., Dauda, T.A., Truman, C.E., Smith, D.J., Memhard, D., Pfeiffer, W., 2006. Predictions and measurements of residual stress in repair welds in plates. Int. J. Press. Vessels Pip. 83 (11–12), 809–818.
Carey, V.P., Mandrusiak, G.D., 1986. Annular film flow boiling of liquids in a partially heated, vertical channel with offset strip fins. Int. J. Heat Mass Transf. 29 (6), 927–939.
Celik, E., Sayman, O., Karakuzu, R., Ozman, Y., 2007. Numerical analysis of the influence of buffer layer thickness on the residual stresses in YBCO/$La_2Zr_2O_7$/Ni superconducting materials. Mater. Des. 28 (7), 2184–2189.
Chang, K.H., Lee, C.H., 2007. Residual stresses and fracture mechanics analysis of a crack in welds of high strength steels. Eng. Fract. Mech. 74 (6), 980–994.
Chen, H., Gong, J., Geng, L., Tu, S.-T., 2006. Numerical analysis of thermal deformation and residual stress for the brazed plate-fin structure. In: ASME 2006 Pressure Vessels and Piping/ICPVT-11 Conference. American Society of Mechanical Engineers, pp. 373–381.
Chena, H., Gonga, J., Genga, L., Tua, S.-T., 2005. Finite element prediction of residual stresses and thermal distortion in a brazed plate-fin structure. J. Press. Equip. Syst. 3, 118–124.
Civalek, O., 2004. Application of differential quadrature (DQ) and harmonic differential quadrature (HDQ) for buckling analysis of thin isotropic plates and elastic columns. Eng. Struct. 26 (2), 171–186.
Galli, M., Botsis, J., Janczak-Rusch, J., 2006. Relief of the residual stresses in ceramic-metal joints by a layered braze structure. Adv. Eng. Mater. 8 (3), 197–201.
Jiang, W.C., Chen, H., Gong, J.M., Tu, S.T., 2011a. Numerical modelling and nanoindentation experiment to study the brazed residual stresses in an X-type lattice truss sandwich structure. Mater. Sci. Eng. A Struct. Mater. Prop. Microstruct. Process. 528 (13–14), 4715–4722.
Jiang, W.C., Gong, J.M., Tu, S.T., 2010. A new cooling method for vacuum brazing of a stainless steel plate-fin structure. Mater. Des. 31 (1), 648–653.
Jiang, W.C., Wang, B.Y., Gong, J.M., Tu, S.T., 2011b. Finite element analysis of the effect of welding heat input and layer number on residual stress in repair welds for a stainless steel clad plate. Mater. Des. 32 (5), 2851–2857.
Jiang, W.C., Yang, B., Gong, J.M., Tu, S.T., 2011c. Effects of clad and base metal

thickness on residual stress in the repair weld of a stainless steel clad plate. J. Press. Vessel Tech. Trans. ASME 133 (6).
Jiang, W.C., Zhang, Y.C., Woo, W., 2012. Using heat sink technology to decrease residual stress in 316L stainless steel welding joint: finite element simulation. Int. J. Press. Vessels Pip. 92, 56–62.
Kim, T.S., Kuwamura, H., 2007. Finite element modeling of bolted connections in thin-walled stainless steel plates under static shear. Thin-Walled Struct. 45 (4), 407–421.
Kong, X., Yang, Q., Li, B., Rothwell, G., English, R., Ren, X.J., 2008. Numerical study of strengths of spot-welded joints of steel. Mater. Des. 29 (8), 1554–1561.
Kuznetsov, V.V., Shamirzaev, A.S., 2007. Boiling heat transfer for freon R21 in rectangular minichannel. Heat Transf. Eng. 28 (8–9), 738–745.
Lee, J.H., 1988. Some Exact and Approximate Solutions for the Modified von Mises Yield Criterion. Preprint - American Society of Mechanical Engineers, November 27, 1988-December 2, 1988. Publ by American Soc of Mechanical Engineers (ASME), Chicago, IL, USA. p WA/APM22 27-WA/APM22 27.
Ligterink, N.E., Hageraats-Ponomareva, S.V., Velthuis, J.F.M., 2012. Mechanical integrity of PFHE in LNG liquefaction process. In: Barrio, M., Venvik, H.J. (Eds.), 2nd Trondheim Gas Technology Conference, pp. 49–55.
Liu, Q., 1997. Modelling the effect of welding residual stresses on fracture toughness of a welded joint. Int. J. Press. Vessels Pip. 72 (2), 103–109.
Liu, Z., Winterton, R., 1991. A general correlation for saturated and subcooled flow boiling in tubes and annuli, based on a nucleate pool boiling equation. Int. J. Heat Mass Transf. 34 (11), 2759–2766.
Ma, H., Cai, W., Yao, Y., Jiang, Y., 2016. Investigation on stress characteristics of plate-fin structures in the heat-up process of LNG heat exchanger. J. Nat. Gas Sci. Eng. 30, 256–267.
Ma, H., Cai, W., Zheng, W., Chen, J., Yao, Y., Jiang, Y., 2014. Stress characteristics of plate-fin structures in the cool-down process of LNG heat exchanger. J. Nat. Gas Sci. Eng. 21 (0), 1113–1126.
Ma, H., Chen, J., Cai, W., Shen, C., Yao, Y., Jiang, Y., 2015. The influence of operation parameters on stress of plate-fin structures in LNG heat exchanger. J. Nat. Gas Sci. Eng. 26, 216–228.
Manglik, R.M., Bergles, A.E., 1995. Heat transfer and pressure drop correlations for the rectangular offset strip fin compact heat exchanger. Exp. Therm. Fluid Sci. 10 (2), 171–180.
Sen, F., Celik, E., Toparli, M., 2007. Transient thermal stress analysis of CeO2 thin films on Ni substrates using finite element methods for YBCO coated conductor. Mater. Des. 28 (2), 708–712.
Xie, Q.Y., Ling, X.A., 2010. Numerical analysis of residual stress for copper base brazed stainless steel plate-fin structure. J. Mater. Eng. Perform. 19 (5), 611–615.